Catalysis Today 150 (2010) 61–66

Contents lists available at ScienceDirect

Catalysis Today

journal homepage: www.elsevier.com/locate/cattod

On the virtue of acid–base titrations for the determination of basic sites in nitrogen doped carbon nanotubes

J.H. Bitter *, S. van Dommele, K.P. de Jong

Inorganic Chemistry and Catalysis, Department of Science, Utrecht University, Sorbonnelaan 16, P.O. Box 80083, 3508 TB Utrecht, The Netherlands

ARTICLE INFO

Article history:
Available online 23 October 2009

Keywords:
NCNT
Surface chemistry
Acid–base titration
Doped carbon nanotubes

ABSTRACT

The basicity and nature of basic species in nitrogen containing carbon nanotubes (NCNT) prepared under different conditions were investigated by acid–base titrations. Proton uptake curves were derived from the titration data and were used to establish the basicity (pK_a) ranges of nitrogen species present in NCNT. Based on the evolution of the titration curves upon acid addition the NCNT were divided into three classes: (I) in which pyridinic type N with a pK_a of 7–9 were predominantly present; these pyridinic groups had some buffering capacity in a pH range of 5–7; (II) where amine type N with a pK_a of 7–9 were the major species; these groups showed only minor buffering capacity at pH 8–9; (III) NCNT with low basicity, i.e. most groups possessed a $pK_a < 7$ with insignificant buffering capacity. All NCNT could be regarded as being composed of organic nitrogen containing building blocks having different pK_a values.

1. Introduction

Carbon nanotubes (CNT) and carbon nanofibers (CNF) are emerging materials which are suitable as catalysts [1,2], catalyst supports [3,4] or as electronic devices [5,6]. One way of altering both the chemical and electronic properties of nanostructured carbon materials is by incorporation of a heteroatom like nitrogen into the graphene sheets resulting in nitrogen containing CNT (NCNT) [6–9]. Recently we have shown that these NCNT materials exhibit activity for the base catalyzed Knoevenagel condensation [9]. However, the nature of the accessible basic sites, relevant for catalysis, is still a matter of debate.

XPS is often used to study the chemical composition, i.e. N/C ratio and the type of nitrogen species present in NCNT [6,10–17]. Since the analysis depth of XPS is several nanometers in carbon materials and, accounting for a graphene layer spacing of about 0.34 nm in CNT, this technique will probe several graphene sheets of NCNT. Therefore, XPS probes both the inaccessible and accessible nitrogen; only the latter is relevant for catalysis. Acid–base titrations on the other hand probe only the accessible sites, which are relevant for catalysis and provides both quantitative and qualitative information concerning the N-sites of the material under examination [18–21]. To get a quantitative picture based on the titration curves, these curves may be converted into a proton-binding isotherm, which relates the tendency of a material to bind protons to the pH of the solution/suspension [21,22]. Subsequently, the proton affinity curve can be deconvoluted in terms of pK_a or pK_b contributions.

Here we will report on acid–base titrations in order to determine the amount and nature of accessible basic sites in NCNT. Titration curves of different NCNT have been compared with those of model compounds such as pyridine, pyrrole and 1-(4-bromobenzyl)pyridiniumbromide, representing models for respectively pyridinic N, pyrrolic N and quaternary N. Also model amines like phenylamine and triethylamine have been included in the study. The contribution of the different nitrogen species to the total basicity of different NCNT will be discussed here.

2. Experimental

2.1. Catalyst preparation and NCNT synthesis

Silica or alumina supported cobalt and nickel growth catalysts with a metal loading of approximately 20% (w/w) were synthesized using Homogeneous Deposition Precipitation [12,23,24]. About 0.5 g of the growth catalyst was loaded in a vertical quartz reactor and reduced to 973 K for 2 h in a 20% H_2/He flow (total 100 ml min^{-1}). Next, the reduced catalyst was kept at its Tamman temperature, i.e. 885 K (Co) or 865 K (Ni), in a helium flow for 1 h. NCNT were grown from acetonitrile (ACN) or pyridine (PYR) at the desired temperature (923 K or 1023 K) by saturating a helium flow (50 ml min^{-1}) with the selected precursor at 303 K. After 16–20 h the growth reaction was stopped by flushing the reactor with helium (50 ml min^{-1}) while cooling to room temperature after which the product was collected.

* Corresponding author.
E-mail address: j.h.bitter@uu.nl (J.H. Bitter).

0920-5861/$ – see front matter © 2009 Elsevier B.V. All rights reserved.
doi:10.1016/j.cattod.2009.09.008

The growth catalyst was removed by subsequently refluxing the raw product in 1 M KOH and 25% HCl solution. The NCNT were thoroughly washed with demiwater after each step. The purified product was dried at 333 K in air. Finally, the material was washed with an NH_4OH solution to remove any salts formed between the basic sites in the NCNT and the acid. Samples were labelled according to metal, temperature and precursor; Co923ACN for example refers to NCNT grown from acetonitrile at 923 K using a cobalt catalyst.

2.2. Quaternarization of pyridine and pyridinic nitrogen in NCNT

Pyridine (1.5 g) was dissolved in a solution of 4-bromobenzylbromide (7.1 g) in toluene (100 ml). The quaternarization reaction was performed under reflux conditions for 1 h. During the reaction a white precipitate was formed. After the reaction, the suspension was cooled to room temperature and filtered. The white precipitate was collected, washed four times with diethylether and dried at room temperature. The product was analyzed with XPS.

Pyridinic nitrogen at the accessible NCNT surface was transformed to quaternary nitrogen by reacting the NCNT with 4-bromobenzylbromide. NCNT (0.65 g) were heated under vacuum to 423 K and maintained at that temperature. After 2 h the NCNT were cooled to room temperature and kept under nitrogen atmosphere. Next, the NCNT were suspended in a 100 ml solution of 4-bromobenzylbromide (2 g) in toluene in such a way that the amount of reactant was two times the amount of nitrogen in the NCNT as determined with XPS analysis. The reaction mixture was heated to reflux and continuously stirred. After 24 h the suspension was filtered and the residue was washed with diethylether four times. The product was dried at room temperature afterwards.

2.3. Characterization

Nitrogen physisorption analysis was conducted using a Micromeretics Tristar 3000 V 6.01 at 77 K. Prior to the analysis the samples were dried at 403 K in a He flow for 14 h.

The morphology of the NCNT was examined by transmission electron microscopy (TEM) using a Tecnai20FEG electron microscope operated at 200 kV. An amount of NCNT was crushed and suspended in ethanol. A drop of the suspension was deposited on to a holey carbon film and the solvent was evaporated.

For acid–base titrations first an electrolyte solution was prepared by dissolving KCl (7.45 g) in 1 l deionized water. A sample of NCNT (0.1 g) was ground and subsequently dried under reduced pressure at 423 K for 1–2 h to remove any adsorbed carbon dioxide. The sample was suspended in the electrolyte solution (70 ml) and stirred for 24 h to reach equilibrium. The suspension was then titrated with a hydrochloric acid solution (2×10^{-3} M) under continuous stirring and under nitrogen atmosphere. The titrations were performed automatically using a Titralab TIM880. The pH was recorded as a function of the amount of titrant added. The rate of the addition was limited to a minimum of 0.2 ml min^{-1} and a maximum of 0.8 ml min^{-1} and in such a way that the pH changes per second were in the interval 0.01–0.05.

The proton uptake by the NCNT as function of suspension pH was calculated using formula (1) [20]:

$$N = V_0C_0 + V_aC_a - (V_0 + V_a) \times 10^{-\mathrm{pH}} \quad (1)$$

where N is the amount of protons absorbed by the NCNT in mol, V_0 and V_a represent respectively the volume of the suspension at start of the titration and the volume of acid added in liters, C_0 and C_a are respectively the concentration of protons in the suspension at start of the titration and concentration of the acid in mol l^{-1}.

The proton uptake was plotted as function of pH and the obtained curves were deconvoluted with Gaussian curves of which the position of the peak's maximum corresponds to the pK_a value of the conjugated acid of a particular basic site on the NCNT surface. The pK_a value of a certain basic site was determined by taking the derivative of the titration curve (pH as function of titrant addition) and locating the maxima of the derivative curve. With the maximum the equivalence point could be found which was then used to find the corresponding pK_a value using the following relationship:

$$\mathrm{p}K_a = \mathrm{pH} \text{ at } V = \frac{1}{2}V_{eq} \quad (2)$$

The pK_a values were used as starting points to fit the proton uptake curve by varying the peak FWHM and position of the maximum within a set limit (ΔpH = 1).

Titration curves of pure nitrogen containing organic compounds were taken as reference. Pyridine (0.01 mmol), 4-methylpyridine (0.01 mmol), quinoline (0.01 mmol), benzylamine (0.004 mmol), piperidine (0.04 mmol) or triethylamine (0.04 mmol) were dissolved in 70 ml of the electrolyte solution. Subsequently these solutions were titrated with hydrochloric acid under continuous stirring and nitrogen flow.

3. Results

Typical transmission electron micrographs a NCNT samples, i.e. Co923ACN is displayed in Fig. 1. The significant contrast between the centre and edge of the material suggests tube morphology and an on-top view (examples indicated with arrows) further proved that the material comprised hollow tubes. For reason of clarity we focus in this paper only on three samples whose distinct different basic properties as will be shown later, i.e. Co923PYR, Co1023ACN and Ni1023ACN. Some of the properties of these samples are compiled in Table 1.

Typical titration curves of these samples are shown in Fig. 2. The initial pH is between 7 and 10 thus showing the NCNT's mildly basic character in aqueous environment. The pH evolution as function of the added amount of HCl is different for the three samples. Co923PYR showed a gradual pH decrease with amount of HCl added while Co1023ACN showed an initial steep decline. Ni1023ACN seemed to display an intermediate behaviour.

The titration curves were converted to proton uptake curves in order to emphasize the variety of basic groups present in the different samples. Fig. 3 shows the proton uptake curves for the different NCNT and their deconvolution using Gaussian type curves with distinct pK_a values. The proton uptake curves have been, in general, fitted with the sum of four Gaussian curves with pK_a values around 4, 6, 7 and 8. The amount of groups within a certain pK_a interval for each sample is reported in Table 2.

Clearly the amount and nature of titratable sites vary with the synthesis parameters of the NCNT.

To get insight in the nature of the basic groups present in NCNT model compounds with sp^3 hybridized N atoms, i.e. triethylamine (pK_a = 10.75), benzylamine (pK_a = 9.33) and piperidine (pK_a = 11.12) and sp^2 hybridized N atoms, viz. quinoline, pyridine and 4-methylpyridine are displayed in Fig. 4. The titration curves of sp^3 hybridized amine compounds started at a pH > 9 and displayed a steep decline, like strong bases, when the equivalence point was reached (Fig. 4A). Despite the fact that the start of the decline is different for each amine, the shape of the titration curve is the same for all amine compounds. Buffering by amines occurred at relatively high pH values, i.e. between 10 and 8, before a fast drop of pH set in.

The evolution of the titration curve sp^2 hybridized molecules such pyridine (Fig. 4B), starting at pH 8, displayed a gradual decline

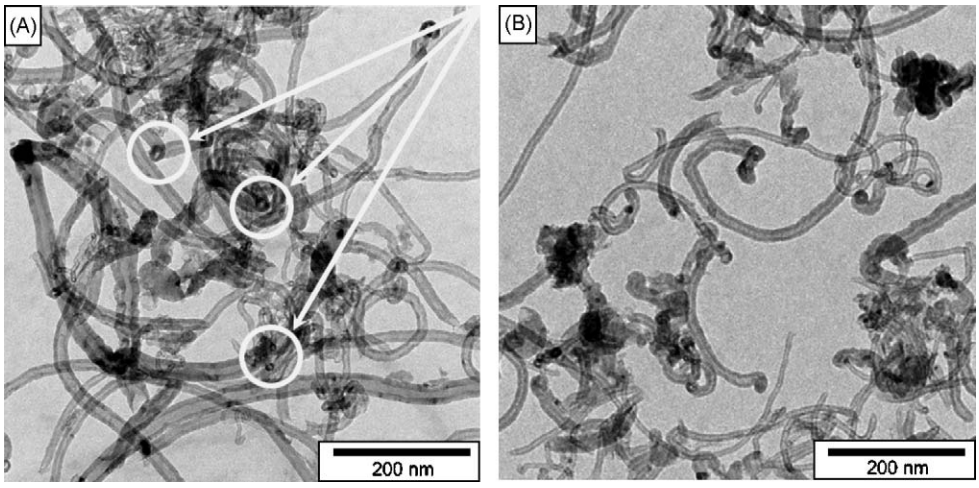

Fig. 1. Transmission electron micrographs of Co923ACN (A) and Ni923ACN (B).

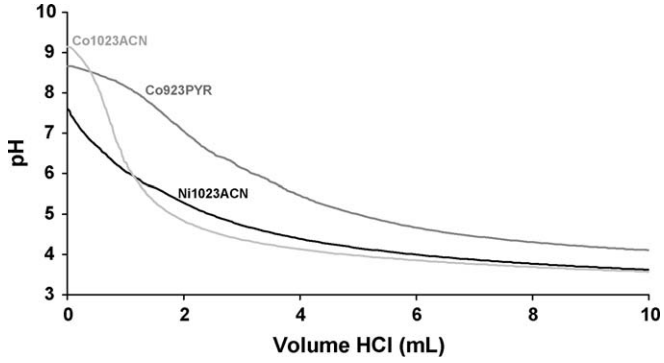

Fig. 2. Titration curves of different NCNT.

with the addition of titrant as opposed to the steep pH drop in the amine titration curves. Buffering of the solution occurred at a lower pH value as compared to amine species but extended to a broad range of titrant addition. This different behaviour of the sp^2 and sp^3 hybridized compounds allows, at least in principle, the deconvolution of a titration curve into their single components.

To verify the influence of pyridinic and quaternary nitrogen on the evolution of the titration curves we compared the titrations curves of equimolar amounts of pyridine before and after quaternarization (Fig. 5A). Also we compared the titration curves of NCNT, with all nitrogen types present before and after quaternarization of the pyridinic nitrogen (Fig. 5B). As can be seen in Fig. 5B quaternarization of the nitrogen atom drastically changes the evolution of the titration curve. While pure pyridine had an initial pH 8 and the solution acidity slowly increased the curve of functionalized pyridine started at $pH < 7$ and then dropped to pH 4 in a small interval of titrant addition. Likewise, the pure NCNT sample, in which every nitrogen type was present, clearly displayed a basic character, starting at pH 9 and gradually being protonated by the addition of acid. The functionalized NCNT on the other hand, with all pyridinic nitrogens converted to quaternary nitrogens, showed no basic character at all.

4. Discussion

4.1. Types of nitrogen

Five types of nitrogen might be present in NCNT, i.e. pyridinic N, pyrrolic N, quaternary N, N-oxide and amine N [6,10–17]. The relative abundance and the chemical environment of these N-types are expected to determine the acid/base properties of the materials as revealed by the titration curves. Therefore, it is imperative to understand the electron donor/acceptor properties of these N-types and their chemical environment. Of these four types the sp^2 hybridized quaternary N, substituting a carbon atom of the graphitic matrix, is under-coordinated and contributes one electron to the conjugated π system of the aromatic carbon matrix [3,12,14]. The result of this is the delocalization of the electrons of the nitrogen atoms. Therefore removing an electron from this nitrogen, i.e. the uptake of H^+ by the nitrogen atom, will decrease the aromaticity of the system which is energetically unfavourable. Therefore, these nitrogens are not expected to display any basic behaviour. Indeed, the material after quaternarization showed no basicity any longer. This result confirms that quaternary nitrogen does not contribute to the basicity of the NCNT.

The sp^3 hybridized nitrogen atom in pyrrole is also part of an aromatic network [6]. Protonation of the nitrogen atom requires electron donation to the H+ ion and results in a loss of aromaticity of the fivefold ring, which is energetically unfavourable. Therefore, pyrrole will have a more acidic character rather than a basic one as was also experimentally established [14].

The N-O species, essentially being an oxidized form of pyridinic N, have been reported to have acidic character [25]. pK_a values below 3 were found for pyridine N-oxides and comparable compounds, determined from protonation experiments.

Pyridinic nitrogen can act as both a Lewis base and a Brønsted base and thus can interact with a proton. Therefore, of all the N-types mentioned above, the pyridinic type nitrogen and amine species are expected to be titrated. From Table 2 it is clear that a broad distribution of groups with different pK_a values are present in the sample. Since the most likely candidates for basicity are only

Table 1
Some properties of the NCNT used in this study.

	Surface area ($m^2 g^{-1}$)	Mesopore volume ($cm^3 g^{-1}$)	pore diameter (TEM) (nm)	Outer tube diameter (TEM) (nm)
Co1023ACN	106	0.49	17	18
Co923PYR	122	0.59	19	18
Ni1023ACN	148	0.52	14	20

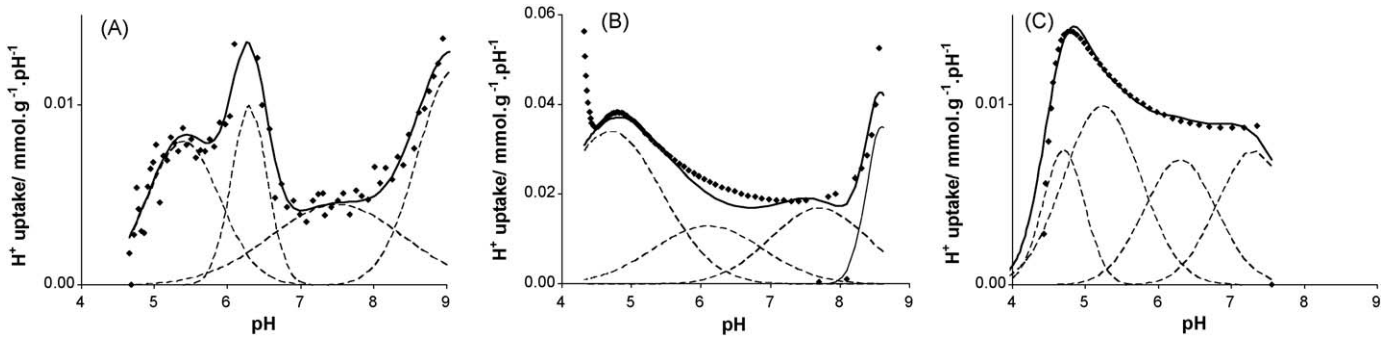

Fig. 3. Proton uptake curves and their fits of (A) Co1023ACN, (B) Co923PYR and (C) Ni1023ACN. Diamonds: raw data, solid line: total fit, dashed lines: individual contributions to the fit.

Table 2
pK_a regions and amount of accessible sites for different NCNT.

	Amount of sites (mmol g^{-1})			
	pK_a: 5–6	pK_a: 6–7	pK_a: 7–8	pK_a: 8–9
Co1023ACN	0.010	0.007	0.010	0.007
Co923PYR	–	0.026	0.029	0.019
Ni1023ACN	0.013	0.009	0.009	–

the pyridinic and amine nitrogen groups the broad distribution of pK_a values must be the result of the different environments in which the nitrogen atoms are located.

4.2. Influence of environment on the properties of pyridinic N

Here we will discuss the influence of the chemical environment of an N atom in NCNT on its base properties. The base properties of different nitrogen containing organic compounds, used as analogues, may aid in a better understanding of the base properties of the N atoms in NCNT. As will be explained, the chemical surrounding of the NCNT's N atom is influenced by the presence of defects in the graphene structure. When NCNT would consist of perfectly ordered graphene layers constructed out of six membered aromatic rings with a random distribution of N atoms, the amount of titrated species would be relatively low, i.e. only at the tube ends pyridinic nitrogen would be found (encircled N atoms in Fig. 6A) which could be titrated. The other N atoms would be quaternary nitrogen. However, when there are defects around the N atoms in the graphene layers more N atoms would be of the NP type as represented schematically by Fig. 6B.

The incorporation of nitrogen into the graphene sheets alters the perfectly ordered aromatic structure which may lead to defects in the NCNT. This could affect the accessibility of the N-sites and thus the amount of groups that are being titrated. Furthermore, the presence of defects around a N-site may also influence the pK_a value of that site. In Table 3 the pK_a value of a number of nitrogen

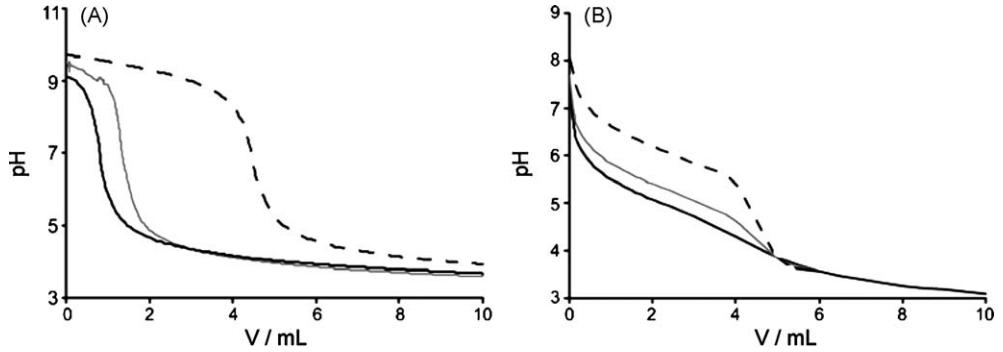

Fig. 4. Titration curve of sp3 hybridized N compounds (A): triethylamine (grey line), benzylamine (dashed line) and piperidine (black line). Titration curve of sp2 hybridized N compounds (B): quinoline (black line), pyridine (grey line) and 4-methylpyridine (dashed line).

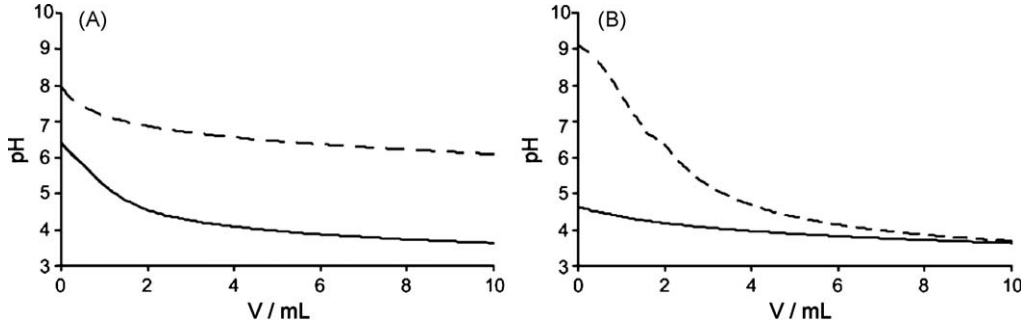

Fig. 5. (A) titration curves of pyridine (dashed line) and 4-bromobenzylpyridinium bromide (solid line). (B) Titration curves of NCNT (Co823ACN) pure (dashed line) and pyridinic N inhibited (solid line).

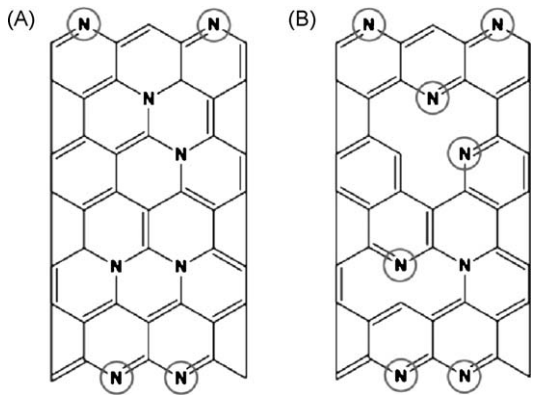

Fig. 6. N atoms in a perfectly ordered graphene layer (A) and N atoms in a graphene layer with defects (B).

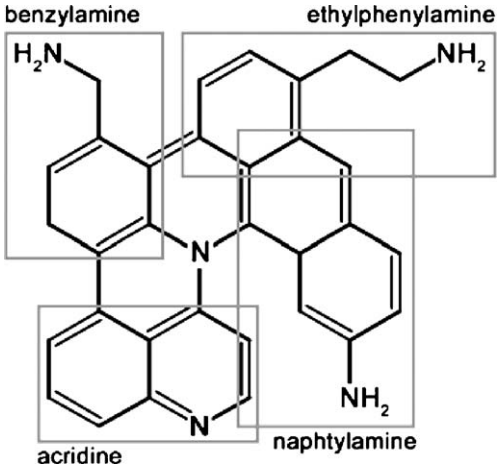

Fig. 7. Nitrogen containing organic molecules as building blocks for NCNT.

containing organic compounds have been compiled with different chemical environments around the N atom. As can be seen from this table an increase of aromatic groups around an sp^3 hybridized N atom causes its pK_a value to decrease, probably caused by the electron withdrawing force exerted by the aromatic groups. If the N atom is separated from the aromatic groups by alkyl chains the pK_a value increases with the increasing number of CH_2 units in the chain. In the same way the pK_a value of an sp^2 hybridized N atom is altered by the presence of aromatic groups. Using these molecules as model building blocks for the NCNT structure (Fig. 7) it can be expected that the local chemical environment around the N atom in the graphene sheets of the NCNT influenced its pK_a value in the same manner as it is influenced by the surrounding groups in the model compounds.

Table 3
pK_a values of N containing organic compounds [26].

Compound	Formula	N hybridization	pK_a	pK class
Methyl-1-naphtylamine	$C_{11}H_{11}N$	sp^3	3.67	3–4
b-Naphtylamine	$C_{10}H_9N$	sp^3	4.16	4–5
Aniline	C_6H_7N	sp^3	4.63	4–5
Quinoline	C_9H_7N	sp^2	4.90	4–5
Pyridine	C_5H_5N	sp^2	5.23	5–6
Acridine	$C_{13}H_9N$	sp^2	5.58	5–6
2-Methylpyridine	C_6H_7N	sp^2	5.68	5–6
3-Methylpyridine	C_6H_7N	sp^2	5.97	5–6
4-Methylpyridine	C_6H_7N	sp^2	6.02	6–7
Benzylamine	C_7H_9N	sp^3	9.33	9–10
Phenylethylamine	$C_8H_{11}N$	sp^3	9.84	9–10
Ethylamine	C_2H_7N	sp^3	10.70	>10
Triethylamine	$C_6H_{15}N$	sp^3	10.75	>10
Diethylamine	$C_4H_{11}N$	sp^3	11.02	>10
Piperidine	$C_5H_{11}N$	sp^3	11.12	>10

When comparing the evolution of the NCNT titration curve with that of model compounds (Fig. 4) some similarities can be found. For example the titration curve of Co1023ACN resemble that of an amine (Fig. 4A), i.e. a start pH of 9 and upon acid addition the pH drop is large, i.e. from 9 to 5 in a small range of titrant addition. Comparing these results with the pK_a values of nitrogen containing organic compounds (Table 3) some conclusions can be made with respect to the chemical composition of the NCNT surface. It is likely that the surface of NCNT with the above mentioned features contained predominantly sp^3 hybridized nitrogen atoms and hardly any of the sp^2 hybridized type. The titration curves of Co923PYR with pK_a sites in the range 7–8 (Table 2) started at a pH around 8 and displayed a more gradual decline in pH. These curves showed more similarity with the titration curves of pyridine-like compounds as displayed in Fig. 4B. Therefore, it is expected that a substantial part of the NCNT surface contains sp^2 hybridized nitrogen. Finally the titration curve of Ni1023ACN curves hardly displayed any basic character at all and mostly resembled a blank titration curve. Therefore, this material did not contain only a minor amount of measurable basic sites.

5. Conclusions

NCNT, synthesized at various conditions were successfully characterized acid–base titrations. Deconvolution of proton uptake curves, derived from titration data, revealed that NCNT consisted of various N-sites with pK_a values between 5 and 9 which varies with the synthesis parameters of the NCNT. The presence of sites with different pK_a values could be explained by visualizing an NCNT as being constructed of organic basic building blocks each having a specific pK_a value. From the evolution of the titration curves three classes were distinguished which were interpreted in terms of abundance of pyridinic- or amine type N present in NCNT. The three classes could be summarized as (I) in which pyridinic type N with a pK_a of 7–9 were predominantly present; these pyridinic groups had some buffering capacity in a pH range of 5–7; (II) where amine type N with a pK_a of 7–9 were the major species; these groups showed only minor buffering capacity at pH 8–9; (III) NCNT with low basicity, i.e. most groups possessed a p$K_a < 7$ with insignificant buffering capacity

Acknowledgements

C. van der Spek is kindly acknowledged for the TEM analysis. This investigation was supported by The Netherlands Organization for Scientific Research, project 700.50.520.

References

[1] N. Keller, N.I. Maksimova, V.V. Roddatis, M. Schur, G. Mestl, Y.V. Butenko, V.L. Kuznetsov, R. Schlögl, Angew. Chem. Int. Ed. 41 (11) (2002) 1885–1888.
[2] D.S. Su, N. Maksimova, J.J. Delgado, N. Keller, G. Mestl, M.J. Ledoux, R. Schlögl, Catal. Today 102–103 (May (15)) (2005) 110–114.
[3] P. Serp, M. Corrias, P. Kalck, Appl. Catal. A 253 (2003) 337–358.
[4] J.H. Bitter, M.K. van der Lee, A.G.T. Slotboom, A.J. van Dillen, K.P. de Jong, Catal. Lett. 89 (1–2) (2003) 139–142.
[5] F. Kreupl, A.P. Graham, G.S. Duesberg, W. Steinhögl, M. Liebau, E. Unger, W. Hönlein, Microelectron. Eng. 64 (2002) 399–408.
[6] C.P. Ewels, M. Glerup, J. Nanosci. Nanotechnol. 5 (9) (2005) 1345–1363.
[7] M. Terrones, W.K. Hsu, H.W. Kroto, D.R.M. Walton, Top. Curr. Chem. 199 (1999) 190–234.
[8] K. Jiang, A. Eitan, L.S. Schadler, P.M. Ajayan, R.W. Siegel, Nano Lett. 3 (3) (2003) 275–277.
[9] S. van Dommele, K.P. de Jong, J.H. Bitter, Chem. Commun. 46 (2006) 4859–4861.
[10] C. Ronning, H. Feldermann, R. Merk, H. Hofsäss, P. Reinke, J.-U. Thiele, Phys. Rev. B 58 (4) (1998) 2207–2215.

[11] F. Le Normand, J. Hommet, T. Szörényi, C. Fuchs, E. Fogarassy, Phys. Rev. B 64 (2001) 1–15, 235416.
[12] S.H. Lim, H.I. Elim, X.Y. Gao, A.T.S. Wee, W. Ji, J.Y. Lee, J. Lin, Phys. Rev. B 73 (2006) 1–6, 045402.
[13] R. Czerw, M. Terrones, J.-C. Charlier, X. Blasé, B. Foley, R. Kamalakaran, N. Grobert, H. Terrones, P.M. Ajayan, W. Blau, D. Tekleab, M. Rühle, D.L. Carroll, Nanoletter 1 (9) (2001) 457–461.
[14] I. Shimoyama, G. Wu, T. Sekiguchi, Y. Baba, J. Electron. Spectrosc. 114–116 (2001) 841–848.
[15] T. Belz, A. Bauer, J. Find, M. Günter, D. Herein, H. Möckel, N. Pfänder, H. Sauer, G. Schulz, J. Schütze, O. Timpe, U. Wild, R. Schlögl, Carbon 36 (5–6) (1998) 731–741.
[16] E. Raymundo-Piñero, D. Cazorla-Amorós, A. Linares-Solano, J. Find, U. Wild, R. Schlögl, Carbon 40 (2002) 597–608.
[17] R. Arrigo, M. Hävecker, R. Schlög, D.S. Su, Chem. Commun. 48 (2008) 4891–4893.
[18] S.S. Barton, M.J.B. Evans, E. Halliop, J.A.F. MacDonald, Carbon 35 (9) (1997) 1361–1366.
[19] A. Contescu, C. Contescu, K. Putyera, J.A. Schwarz, Carbon 35 (1) (1997) 83–94.
[20] N. Tantavichet, M.D. Pritzker, C.M. Burns, J. Appl. Polym. Sci. 81 (2001) 1493–1497.
[21] K. László, K. Josepovits, E. Tombácz, Anal. Sci. 17 (2001) 1741–1744.
[22] A. Contescu, M. Vass, C. Contescu, K. Putyera, J.A. Schwarz, Carbon 36 (3) (1998) 247–258.
[23] M.K. van der Lee, A.J. van Dillen, J.H. Bitter, K.P. de Jong, J. Am. Chem. Soc. 127 (2005) 13573–13582.
[24] G.L. Bezemer, P.B. Radstake, U. Falke, H. Oosterbeek, A.J. van Dillen, K.P. de Jong, J. Catal. 237 (2006) 152–161.
[25] M. Balón, M.C. Carmona, M.A. Muñoz, J. Hidalgo, Tetrahedron 45 (23) (1989) 7501–7504.
[26] R.C. Weast, Handbook of Chemistry and Physics, 75th ed., CRC Press, Boca Raton, FL, USA. page D159–D161.